AD NUMBER

AD862137

NEW LIMITATION CHANGE

TO

Approved for public release, distribution unlimited

FROM

Distribution authorized to U.S. Gov't. agencies and their contractors; Critical Technology; OCT 1969. Other requests shall be referred to Commanding Officer, Army Aberdeen Research and Development Center, Aberdeen Proving Ground, MD 21005-5066.

AUTHORITY

BRL ltr dtd 22 Apr 1981

BRL

AD

MEMORANDUM REPORT NO. 2013

ANALYSIS OF FREE FLIGHT TESTS OF 107MM MORTAR PROJECTILE XM 571 RAC

by

W. Donovan

October 1969

U.S. ARMY ABERDEEN RESEARCH AND DEVELOPMENT CENTER
BALLISTIC RESEARCH LABORATORIES
ABERDEEN PROVING GROUND, MARYLAND

BALLISTIC RESEARCH LABORATORIES

MEMORANDUM REPORT NO. 2013

OCTOBER 1969

ANALYSIS OF FREE FLIGHT TESTS OF 107MM MORTAR PROJECTILE XM 571 RAC

W. Donovan

Exterior Ballistics Laboratory

RDT&E Project No. 1T262301A201

ABERDEEN PROVING GROUND, MARYLAND

Destroy this report when it is no longer needed.
Do not return it to the originator.

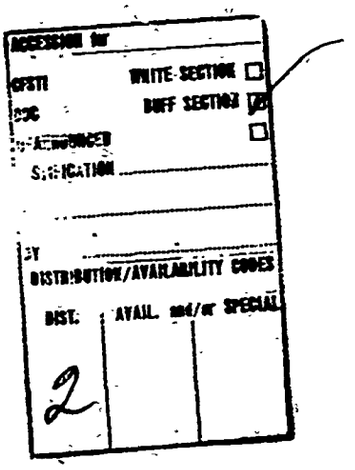

The findings in this report are not to be construed as an official Department of the Army position, unless so designated by other authorized documents.

B A L L I S T I C R E S E A R C H L A B O R A T O R I E S

MEMORANDUM REPORT NO. 2013

WDonovan/1a
Aberdeen Proving Ground, Md.
October 1969

ANALYSIS OF FREE FLIGHT TESTS OF 107MM MORTAR PROJECTILE XM 571 RAC

ABSTRACT

Free flight aerodynamic range data are presented for the 107mm XM 571 RAC mortar projectile in unboosted configuration. Seven different models were tested and most of the data was obtained for the square base shell with extension. For $M \sim 0.8$ and within the small yaw region, this projectile developed a quintic Magnus moment. It was established that the length of the base attachment (extension) directly influenced the values of the aerodynamic coefficients.

TABLE OF CONTENTS

LIST OF ILLUSTRATIONS

LIST OF TABLES

PRECEDING PAGE BLANK

LIST OF SYMBOLS

C_D $= \dfrac{\text{Drag Force}}{(\frac{1}{2})\ \rho\ V^2\ S}$

C_{D_o} = Zero-yaw drag coefficient

$C_{D_{\delta^2}}$ = Yaw drag coefficient

C_{L_α} $= \dfrac{\text{Lift Force}}{(\frac{1}{2})\ \rho\ V^2\ S\ \delta}$ Positive coefficient: Force acts in the direction of the angle of attack α_t, and $\delta = \sin \alpha_t$.

C_{M_α} $= \dfrac{\text{Static Moment}}{(\frac{1}{2})\ \rho\ V^2\ S\ d\ \delta}$ Positive coefficient: Moment increases angle of attack α_t.

$C_{M_{p_\alpha}}$ $= \dfrac{\text{Magnus Moment}}{(\frac{1}{2})\ \rho\ V^2\ S\ d\ \frac{pd}{V}\ \delta}$ Positive coefficient: Moment rotates projectile nose in direction of spin.

For most exterior ballistic uses, where $\dot{\alpha} = q$, $\dot{\beta} = -r$, the definition of the damping moment sum is equivalent to:

$C_{M_q} + C_{M_{\dot{\alpha}}}$ $= \dfrac{\text{Damping Moment}}{(\frac{1}{2})\ \rho\ V^2\ S\ d\ \frac{q_t\ d}{V}}$ Positive coefficient: Moment increases angular velocity.

α, β = angle of attack, side slip

α_t $= \sin^{-1}(\alpha^2 + \beta^2)^{\frac{1}{2}}$, total angle of attack $\sin \overline{\alpha}_t = \sqrt{\overline{\delta^2}}$

c.m. = center of mass

d = body diameter of projectile, reference length

I_x = axial moment of inertia

I_y = transverse moment of inertia

M = Mach number

p = roll rate

r = transverse angular velocities

q_t $= (q^2 + r^2)^{\frac{1}{2}}$

LIST OF SYMBOLS (Continued)

(3) $(C_M)_{Static} = (C_{M_{\alpha_o}} + c_2 \delta^2)\ \delta$

(4) $(C_M)_{Magnus} = (\hat{c}_o + \hat{c}_2 \delta^2 + \hat{c}_4 \delta^4 + ...)\ \delta\ (\frac{p\ d}{V})$

(5) $C_{M_q} + C_{M_{\dot{\alpha}}} = (C_{M_q} + C_{M_{\dot{\alpha}}})_o + d_2 \delta^2$

where $\delta = \sin \alpha_t$

Relations between the coefficients from the linearized fit and the aerodynamic coefficients for the above cases:

(1a) $(C_D)_R = C_{D_o} + C_{D_{\delta^2}} \delta^2$

(2a) $(C_{L_\alpha})_R = C_{L_{\alpha_o}} + a\ (\delta^2)_{eP}$

(3a) $(C_{M_\alpha})_R = C_{M_{\alpha_o}} + c_2\ (\delta^2)_{eN}$

(4a) $(C_{M_{p_\alpha}})_R = C_{M_{p_{\alpha_o}}} + \hat{c}_2\ (\delta^2)_e + \hat{c}_4\ (\delta^4)_e$ (Only nonlinear Magnus)

(5a) $(C_{M_q} + C_{M_{\dot{\alpha}}})_R = (C_{M_q} + C_{M_{\dot{\alpha}}})_o + \hat{c}_2\ (\delta^2)_{e*} + \hat{c}_4\ (\delta^4)_{e*}$ (Only nonlinear Magnus)

and

$$\overline{\delta^2} \approx K_N^2 + K_P^2$$

$$(\delta^2)_{eN} = K_N^2 + 2\ K_P^2$$

$$(\delta^2)_{eP} = 2\ K_N^2 + K_P^2$$

$$(\delta^4)_{eN} = K_N^4 + 6\ K_N^2\ K_P^2 + 3\ K_P^4$$

$$(\delta^4)_{eP} = 3\ K_N^4 + 6\ K_N^2\ K_P^2 + K_P^4$$

$$(\delta^2)_e = K_N^2 + K_P^2 + \frac{\phi_N'\ K_N^2 - \phi_P'\ K_P^2}{\phi_N' - \phi_P'}$$

LIST OF SYMBOLS (Continued)

S = $\frac{\pi d^2}{4}$, reference area

V = velocity of projectile

m = mass of projectile

Stability and Data Reduction Parameters

K_N = amplitude of nutational yaw component

K_P = amplitude of precessional yaw component

ϕ'_N = nutational yaw rate--rad/cal

ϕ'_P = precessional yaw rate--rad/cal

λ_N = nutational damping rate--1/cal

λ_P = precessional damping rate--1/cal

σ_{fit} = standard deviation--$^{\circ}$/cal

Subscripts

i = N or P as indicated in the term expansion

N = nutational component

P = precessional component

R = range value

o = zero-yaw or first term of expansion

2 = second power term of expansion

4 = fourth power term of expansion

Nonlinear Force-Moment Relations

Assumed form of force and moment coefficient relations:

(1) $C_D = C_{D_o} + C_{D_{\delta^2}} \delta^2$

(2) $(C_L) = (C_{L_{\alpha_o}} + a\,\delta^2)\,\delta$

LIST OF SYMBOLS (Continued)

$$(\delta^4)_e = K_N^4 + 6\,K_N^2\,K_P^2 + K_P^4 + 2\left(\frac{\phi_N'\,K_N^4 - \phi_P'\,K_P^4}{\phi_N' - \phi_P'}\right)$$

$$(\delta^2)_{e*} = \frac{I_y}{I_x}\,\frac{(\phi_N' + \phi_P')\,(K_N^2 - K_P^2)}{(\phi_P' - \phi_N')}$$

$$(\delta^4)_{e*} = 2\,\frac{I_y}{I_x}\,\frac{(\phi_N' + \phi_P')\,(K_N^4 - K_P^4)}{(\phi_P' - \phi_N')}$$

1. INTRODUCTION

The XM 571 is a spin stabilized, rocket assisted, HE projectile proposed for use in the 107mm mortar. The test shell represents an attempt to make a major improvement in range performance with the 107mm mortar system. In addition to the rocket boost feature it also had a low drag shape with a long ogival nose, Figure 1, which would provide a higher critical Mach number. These features, however, decrease the stability level of the shell and, as a result, the XM 571 was designed for use with a 1/18 twist tube rather than the twist of 1/20 employed with the current shell, the M 329 shown in Figure 2. Other features of the revised mechanical design include a pre-engraved rotating band and a discarding plastic obturator.

The 107mm mortar is muzzle loading and a cylindrical cartridge container extending from the base of the shell is used to position the shell in the breech of the mortar and provide a powder chamber volume. The cylindrical container is retained in flight. One of the previous improvements employed with the M 329 shell, and incorporated into the design of the XM 571, is the use of an extension to the cartridge container for use with higher powder charges. The use of the extension results in a total cylindrical protuberance about 0.3 caliber in diameter and 1.5 calibers long. In the case of the M 329 it was discovered that the extended cylindrical section produced aerodynamic changes and in particular decreased the gyroscopic and dynamic stability.

The phenomena involved in the change of aerodynamic properties due to the cylindrical attachment was not well enough understood to predict the changes that might occur for another configuration. As a result, spark range tests were carried out with the XM 571 shell at an earlier stage of the development than usual. The series of tests reported involved only unboosted projectiles. Most of the tests were conducted with a square base design that was of primary interest, but screening tests were also conducted with several other configurations. The object of the tests was to evaluate the aerodynamic characteristics with particular attention to those changes which occurred when the base was modified.

Type D

Figure 1. XM 571 RAC Mortar Projectile

II. PROCEDURE

The 107mm mortar tube was set-up outside the transonic range[5] mounted in a 105 M3A1 howitzer carriage, Figure 3, and aligned to fire horizontally through the instrumented section of the range. In addition to the regular shadowgraph stations within the range, two photographic stations were placed three feet and eleven feet from the muzzle outside the range and one station was placed 20 feet from the muzzle and immediately inside the range opening. These stations were located to record the development of the yaw, particularly the yawing rate, and to aid in the analysis of the effects of the muzzle blast. Inside the range, a mosaic station was employed to obtain fine detail shadowgraphs on selected rounds.

The aerodynamic tests consist of free flight evaluation of the inert projectiles at two Mach number conditions, $M \sim .5$ and $M \sim .8$. Variations in base configuration, as catalogued in Table I, include:

a. Square base or boat tail.

b. Extension, cartridge container alone, or without cartridge container.

c. Different arrangements of obturator; large, small, and with and without pressure plate.

d. Rounds with long thin starting cartridge containers.

The square base projectile with extension represents one-half of the number of data rounds fired. Geometric modifications of the shell base and appendage, principally boattailing with and without extension, accounted for the remainder of the data. The aerodynamic coefficients were obtained by the standard reduction techniques[6] using the measurements from the shadowgraphs and corresponding times from the electronic counters.

Physical dimensions and mass moments of inertia of the rounds were measured[3] prior to firing. A photograph of the unfired projectiles illustrating the different cartridge containers and extensions is presented as Figure 4. The physical dimensions, weights and moments of

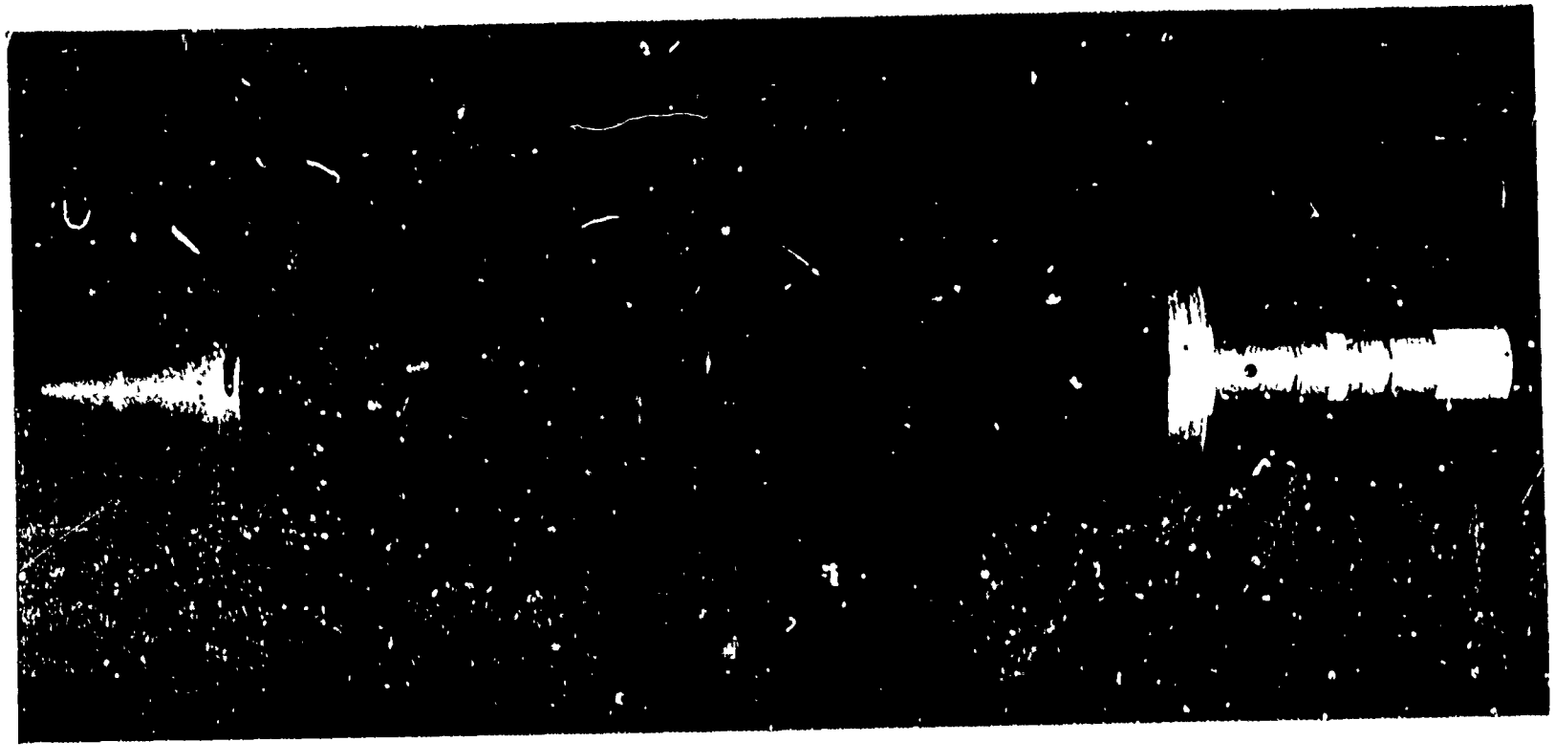

Figure 2. M 329 Mortar Projectile

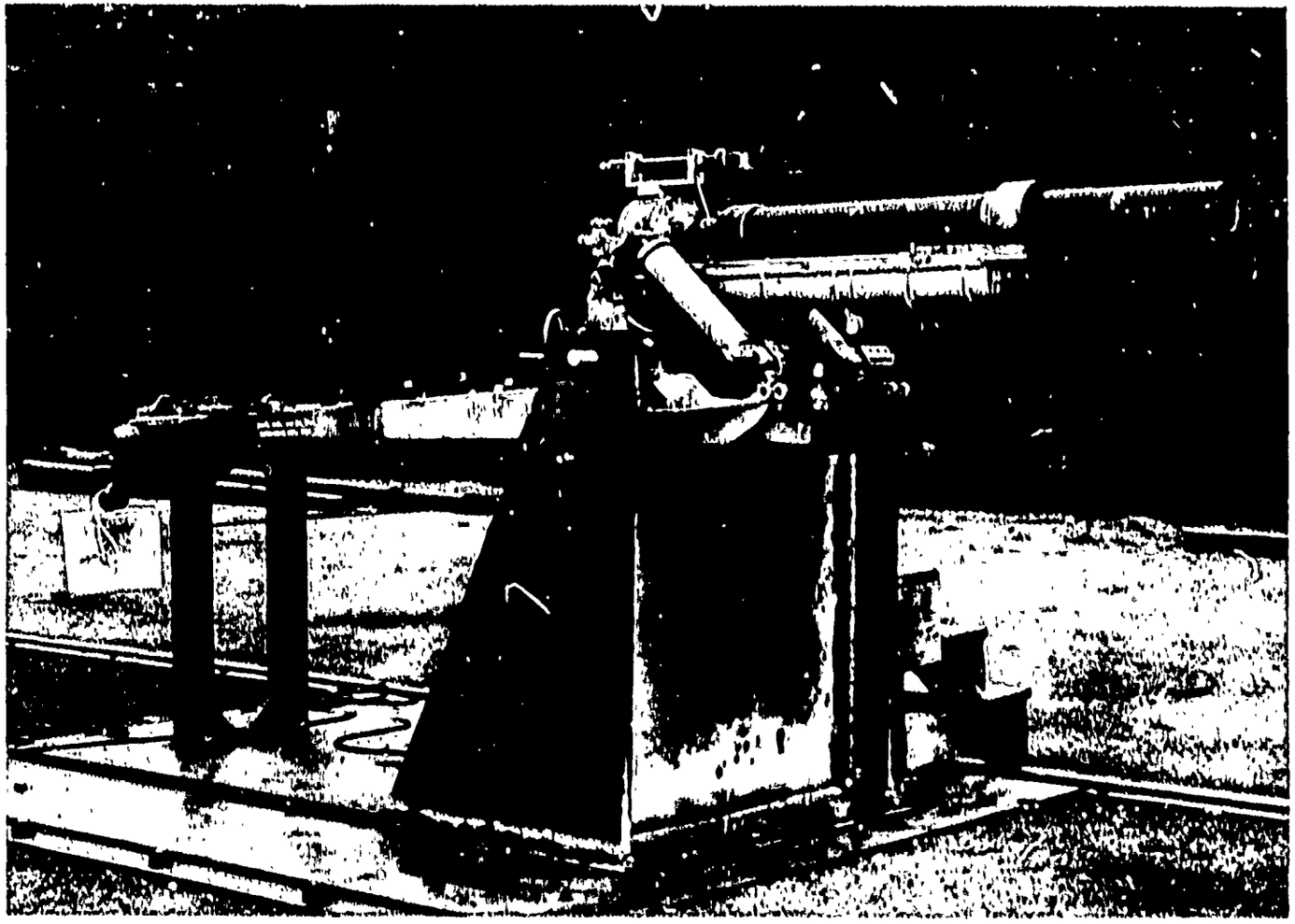

Figure 3. Set-Up of Launch Platform

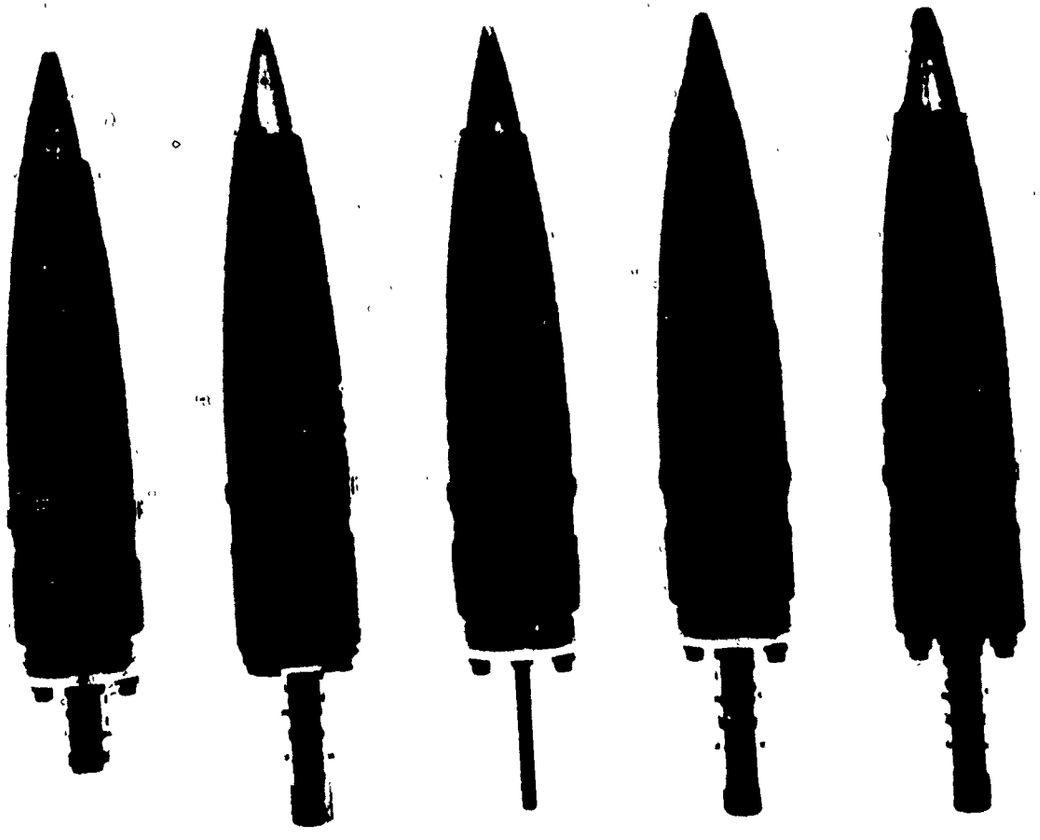

Type E | Type A-B | Type G | Type D-F | Type C

Figure 4. Photographs of Projectiles

inertia are given on Figure 5, and Figure 6 is a dimensioned sketch of the projectile on which most of the data was collected.

III. RESULTS

The results are given in Table II, the Table of Aerodynamic Coefficients, and the drag, static moment and dynamic coefficients are discussed in separate context in following sections. Figures 7, 8 and 9 are photographs of the projectile at the three added photo stations outside and just inside the range entrance. Measurements of these photos were not used nor were they required for the determination of the aerodynamic coefficients but the pictures clearly indicate that the obturator has been discarded within three feet of the muzzle of the mortar. The initial yaw information was of relatively low reliability and the effort to pursue a detailed analysis of the muzzle blast effect had to be abandoned.

The mosaic, Figure 10, shows a boat tail round carrying an extension. The flow in the region of the base is generally disturbed, with boundary convergence developing along the length of the cartridge container and extension and a recirculation region extending within .4 caliber to the base of the shell. With this design, the axial and radial pressures in the near wake act on the cartridge container and extension and produce forces which are critical to the determination of the Magnus and damping characteristics of the projectile. No free flight measurements of the pressure gradients are presently available.

Except for the limited Mach number range, the results define the aerodynamic properties of the configuration with square base carrying an extension. The individual data for the shell with modifications are also reliable but the restricted coverage prevents any clear definition of their properties, either as a function of yaw or of Mach number. In Table II, the length of the swerve arms for Rounds 8203 and 8439 is too small to establish reliable values of C_{L_α}. The damping moment and

The following table lists the variations in shell configuration. Reference 5 and Figures 4 and 5 further describe the modifications of the test projectiles. All rounds were pre-engraved to accommodate the 1/18 twist of the mortar tube. All obturators were made of hard plastic.

Table I. Projectile Description

Type	Lot Number **	Number of Rounds Fired	Aft Body Shape		Pressure Plate	Obturator		Starting Cartridge			
			Boat tail	Square base		Large	Small	Short	With Extension	Thin	None
A	56124	17		x	Yes		x		x		
B	56124	4		x	Yes		x	x			
C	56127	2		x	No						x
D	56126	4	x		No	x			x		
E	56123	2	x		No	x		x			
F	56126	2	x		No	x					x
G	56125	3	x		No	x				x	

** Refers to Picatinny Arsenal designation.

Table II. Table of Aerodynamic Coefficients

** Negative sign on λ indicates damping. **** Test values not reported due to small arm.

*** Drag data for this round not reported due to timing station distribution.

	Type Projectile	Round Number	Mach Number	C_D	$\bar{\alpha}_t$	C_{L_α}	C_{M_α}	$C_{M_q}+C_{M_{\dot{\alpha}}}$	$C_{M_{p\alpha}}$	K_N	K_P	$\lambda_{N_{**}}$	$\lambda_{P_{**}}$	ϕ'_N	ϕ'_P
					deg.							1/cal x 10^4	1/cal x 10^4	rad/cal x 10^2	rad/cal x 10^2
Square Base	A	8211	.826	.222	5.1	1.75	3.84	- 4.6	.13	.069	.056	- .59	-1.43	2.21	.45
	With	8229	.823	.199	4.1	1.64	3.85	- 6.1	.33	.052	.048	- .04	-2.28	2.17	.45
	Extension	8212	.817	.232	5.9	1.92	3.84	- 5.8	.08	.074	.072	-1.19	-1.22	2.23	.45
		8198	.814	.209	4.9	1.89	3.92	- 5.0	.10	.065	.055	- .84	-1.33	2.19	.46
		8223	.812	.213	4.7	1.99	3.93	- 7.0	.17	.064	.056	-1.09	-1.61	2.23	.45
		8199	.809	.222	5.7	1.84	3.85	- 6.9	.07	.069	.072	-1.57	-1.02	2.19	.45
		8201	.809	.210	4.6	2.01	3.94	- 6.8	.25	.061	.050	- .60	-2.10	2.20	.46
		8213	.808	.216	5.4	1.89	3.90	- 4.7	.09	.069	.064	- .81	-1.29	2.21	.45
		8217	.807	.224	5.6	1.86	3.87	- 5.5	.11	.072	.064	- .91	-1.33	2.20	.44
		8197	.805	.206	4.1	1.56	3.92	- 2.7	.32	.061	.042	+1.01	-2.42	2.21	.45
		8216	.803	.217	5.0	1.96	3.90	- 5.6	.06	.063	.060	-1.22	-1.12	2.22	.45
		8224	.799	.199	3.7	1.77	3.92	- 1.3	.16	.053	.038	+ .60	-1.75	2.22	.45
		8222	.798	.244	7.4	1.80	3.88	- 6.7	-.01	.089	.091	-1.93	- .63	2.26	.43
		8203	.531	.185	2.6	****	4.22	-15.4	1.69	.043	.012	+4.34	-8.78	2.16	.49
		8206	.527	.190	3.1	1.37	4.14	- 5.5	.66	.046	.027	+1.99	-4.06	2.16	.49

Table II. Table of Aerodynamic Coefficients (Continued)

	Type Projectile	Round Number	Mach Number	C_D	$\bar{\alpha}_t$	C_{L_α}	C_{M_α}	$C_{M_q}+C_{M_{\dot{\alpha}}}$	$C_{M_{p\alpha}}$	K_N	K_P	$\lambda_{N_{**}}$	$\lambda_{P_{**}}$	ϕ'_N	ϕ'_P
					deg.							1/cal x 10^4	1/cal x 10^4	rad/cal x 10^2	rad/cal x 10^2
Square Base	A With Extension	8205	.523	.269	9.1	1.69	3.55	- 6.4	.35	.127	.094	- .03	-2.38	2.23	.41
		8204	.518	.182	2.3	1.51	4.22	- .2	.67	.034	.018	+3.92	-4.69	2.14	.51
	B Without Extension	8207	.573	***	2.9	1.86	3.07	- 2.8	-.12	.029	.040	-1.26	- .39	2.47	.34
		8209	.518	.192	1.0	2.08	3.08	- 9.0	.16	.004	.016	-1.86	-1.51	2.44	.34
		8210	.516	.227	4.8	1.85	3.07	- 4.5	.03	.053	.065	-1.12	- .98	2.49	.34
		8208	.513	.204	2.9	2.15	3.07	- 7.5	.09	.036	.034	-1.71	-1.29	2.46	.34
	C Without Cartridge Container	8234	.723	.267	6.3	1.97	2.98	- 3.5	-.05	.073	.082	-1.19	- .74	2.59	.33
		8231	.714	.296	8.0	1.94	2.97	- 4.1	.00	.099	.099	-1.29	- .91	2.58	.32
Boat Tail Base	D With Extension	8225	.808	.196	6.8	1.70	4.36	- 7.3	-.15	.073	.091	-3.04	+ .31	2.21	.51
		8436	.801	.179	5.2	1.58	4.45	-10.4	.14	.054	.072	-2.66	- .95	2.16	.56
		8226	.737	.137	1.0	1.48	4.47	****	****	.006	.006	****	****	2.13	.54
		8439	.517	.153	2.0	****	4.65	- 3.5	.67	.032	.010	+3.39	-5.00	2.07	.61
	E Without Extension	8435	.770	.174	4.0	1.90	3.52	- 3.1	.05	.049	.048	- .59	-1.22	2.44	.42
		8438	.501	.160	1.6	1.77	3.43	- 6.3	-.04	.024	.015	-2.21	- .44	2.46	.40

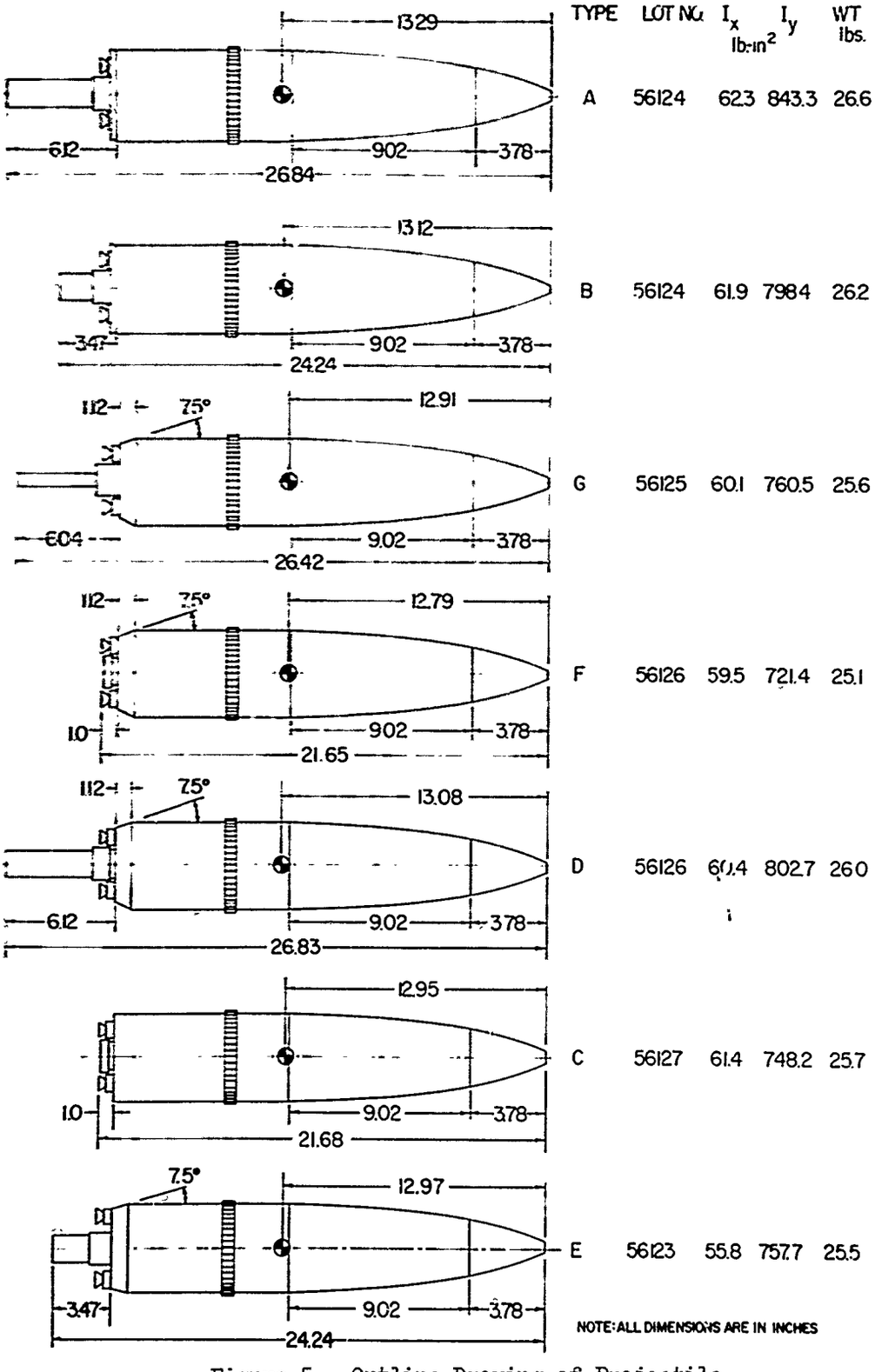

Figure 5. Outline Drawing of Projectile

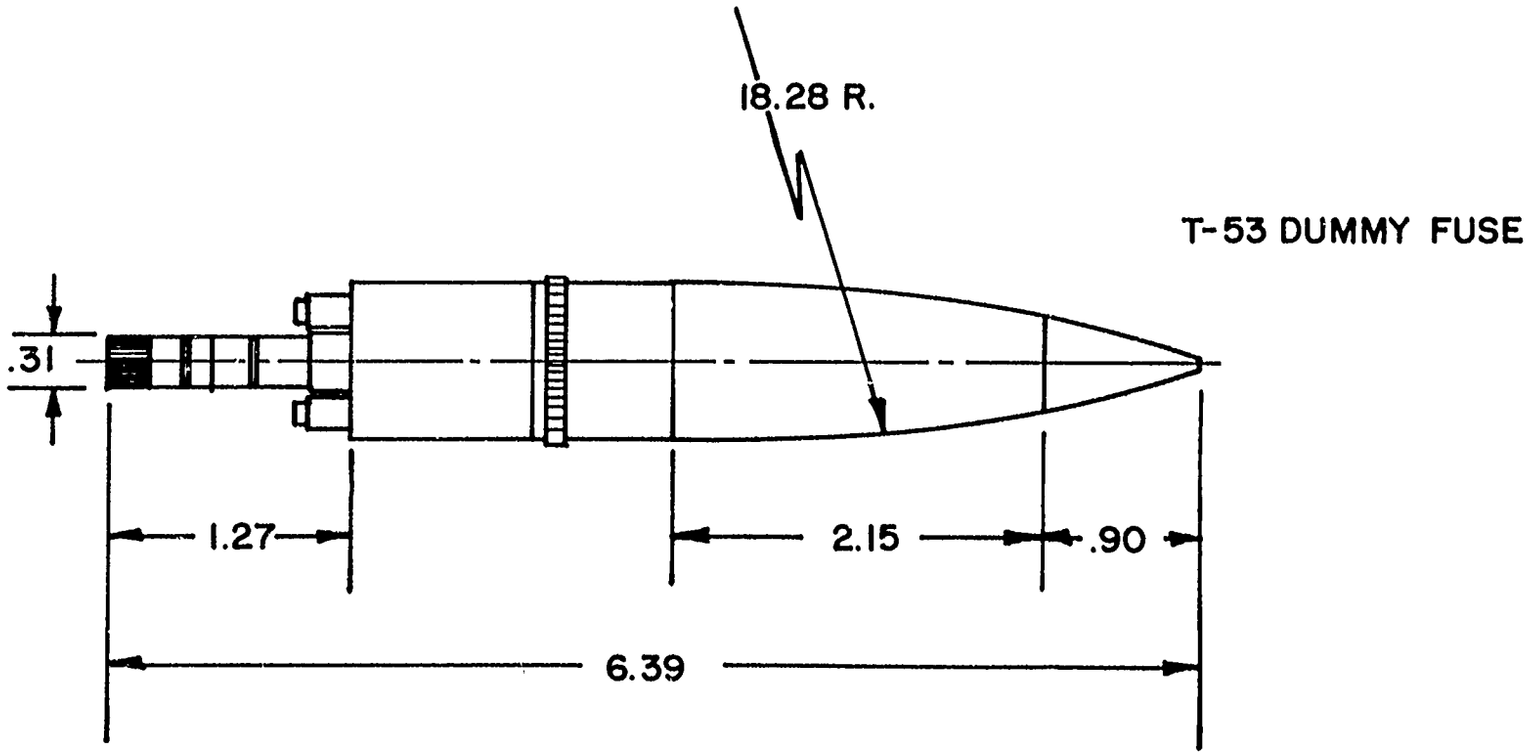

Figure 6. Dimensional Sketch -- Type A

Figure 7. Streak Photograph, Round 8235, .9144 Meters from Muzzle

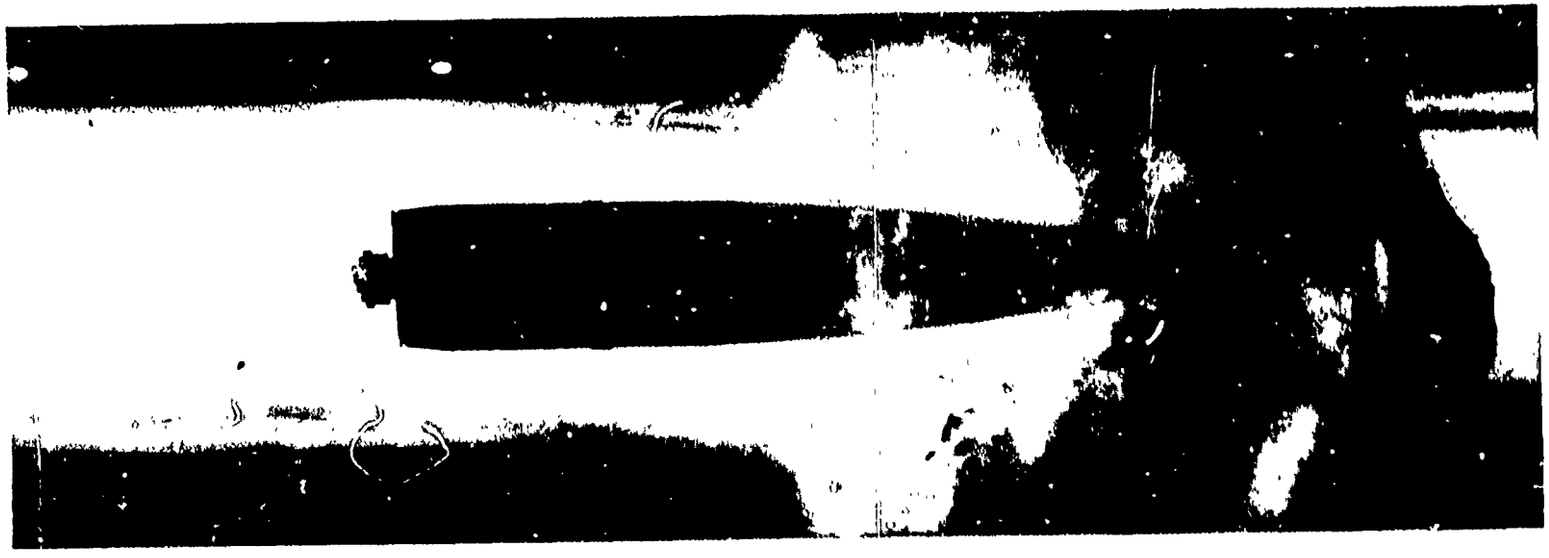

Figure 8. Streak Photograph, Round 8235, 3.3528 Meters from Muzzle

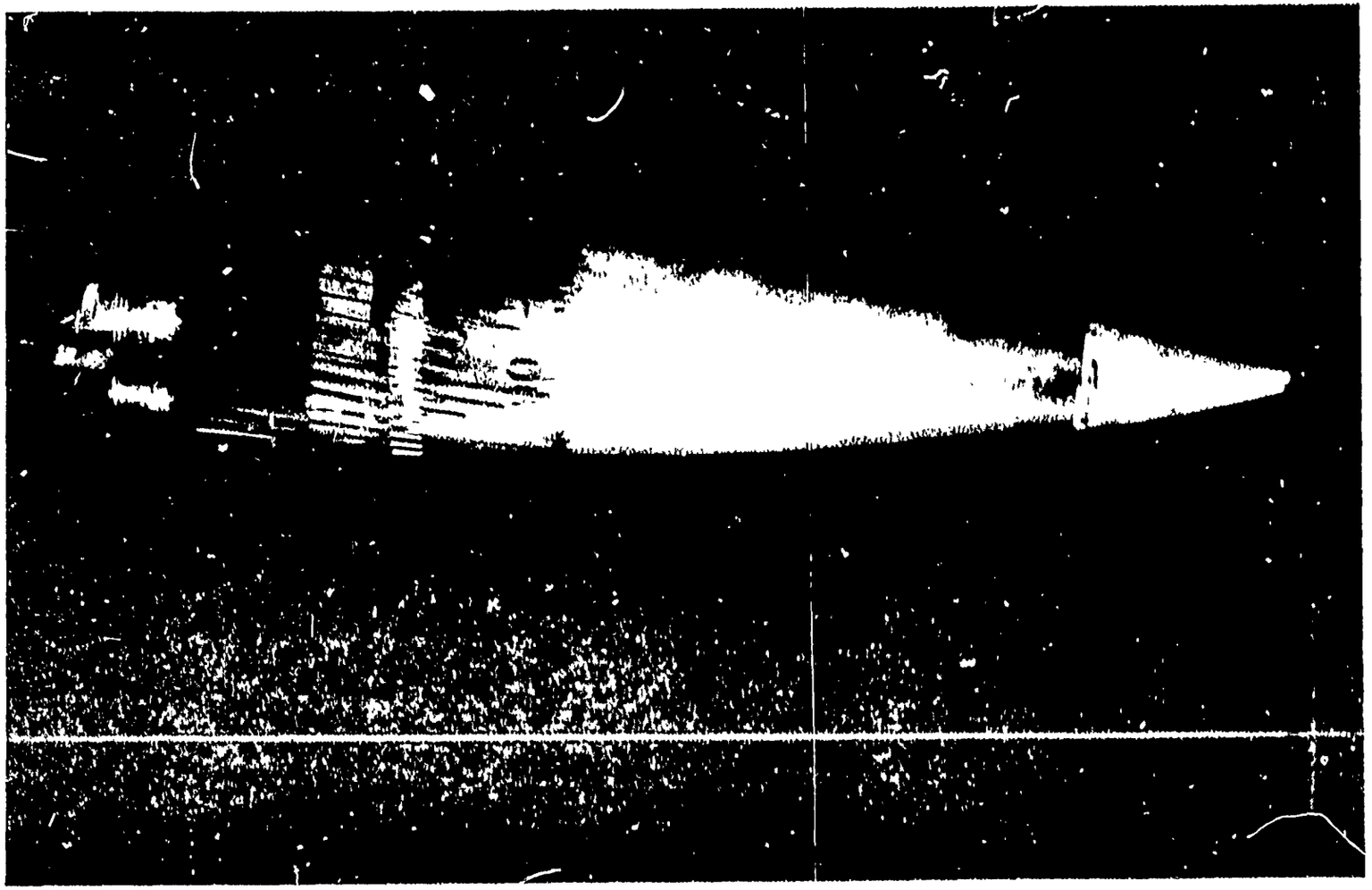

Figure 9. Streak Photograph, Round 8235, Range Entrance

Magnus moment coefficients are reported, although their values depend on C_{L_α}, since they appear to be consistent with corresponding data.

A. Drag

The drag coefficient, C_D, is plotted versus $\overline{\delta^2}$, the mean squared yaw, on Figures 11 and 12. C_D was obtained for each round from a least squares fit of time as a cubic in distance. For each configuration, the data was then reduced to a C_{D_o} by the expression[12]:

$$C_D = C_{D_o} + C_{D_{\delta^2}} \overline{\delta^2} \qquad (1)$$

where $C_{D_{\delta^2}}$ is the yaw drag coefficient. C_D usually changes with Mach number and several test points at different yaws per Mach range investigated are required to determine C_{D_o} and $C_{D_{\delta^2}}$. Even a two point determination is often reasonable considering the high precision of the electronic timing equipment and the transonic range station survey[6]. The overall accuracy of the determination of C_D is within less than 1% error.

Mach number effects were not firmly established since the program was not intended to provide a distribution in test velocity. However, the yaw slope ($C_{D_{\delta^2}}$) is shown on Figures 11 and 12. $C_{D_{\delta^2}}$ for the square base projectiles with extension was found by linear least squares fit to be equal to $4.6/\text{rad}^2$ for the $M \sim .8$ data. The yaw slopes for the other data were determined graphically. There is a change in the yaw slope in Figure 11 and Figure 12 for $\alpha_t > 6°$. However, $C_{D_{\delta^2}}$ for these higher yaw values cannot be established without additional data in this range.

Lower drag coefficients were associated with (1) boat tailing, (2) the addition of the large diameter cartridge container, and (3) the extension attachment. Boat tail projectiles with the thin boom showed a C_D value between the projectiles without extension and those with no base appendage except the rocket nozzles.

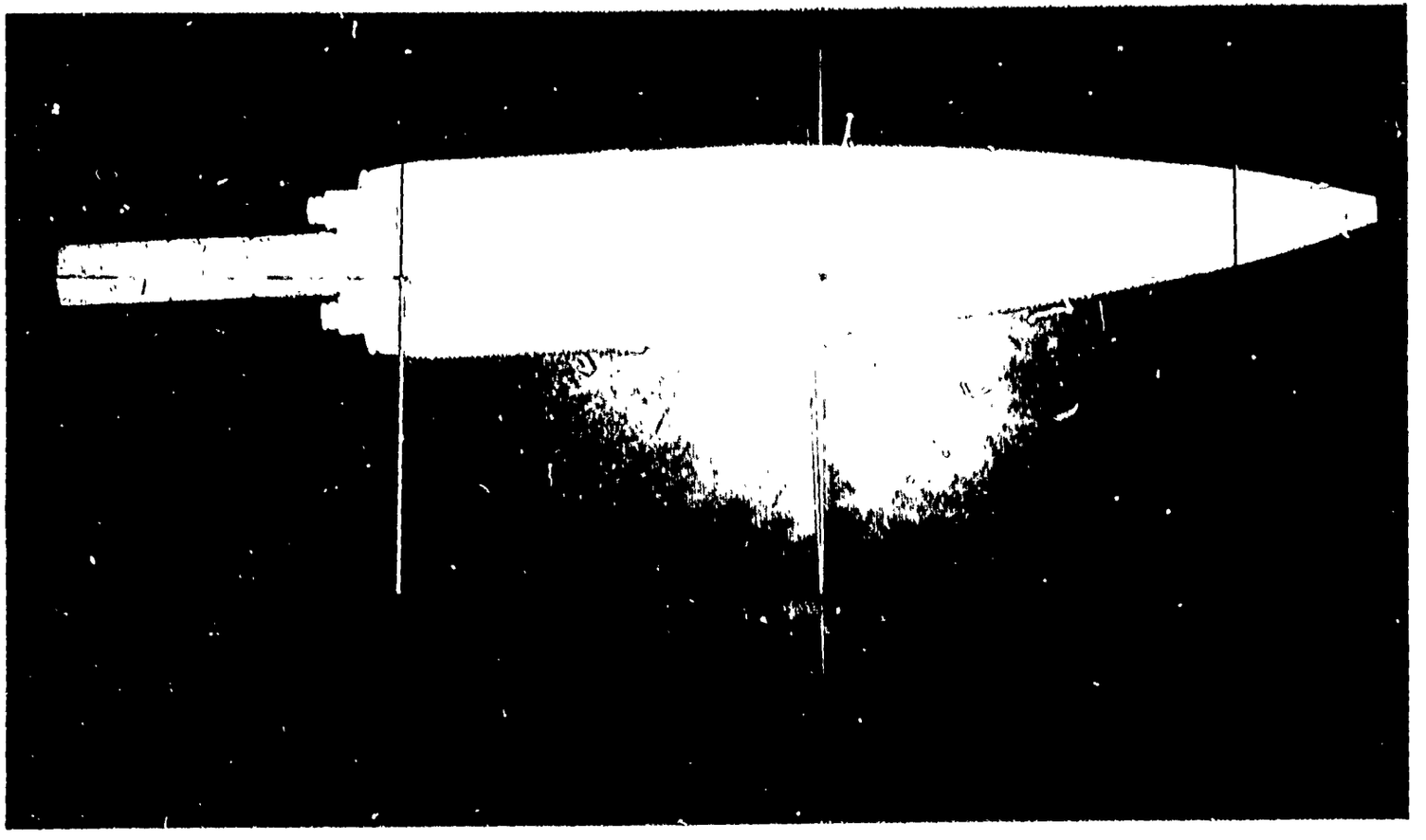

Figure 10. Mosaic, Round 8436, M ~ .8

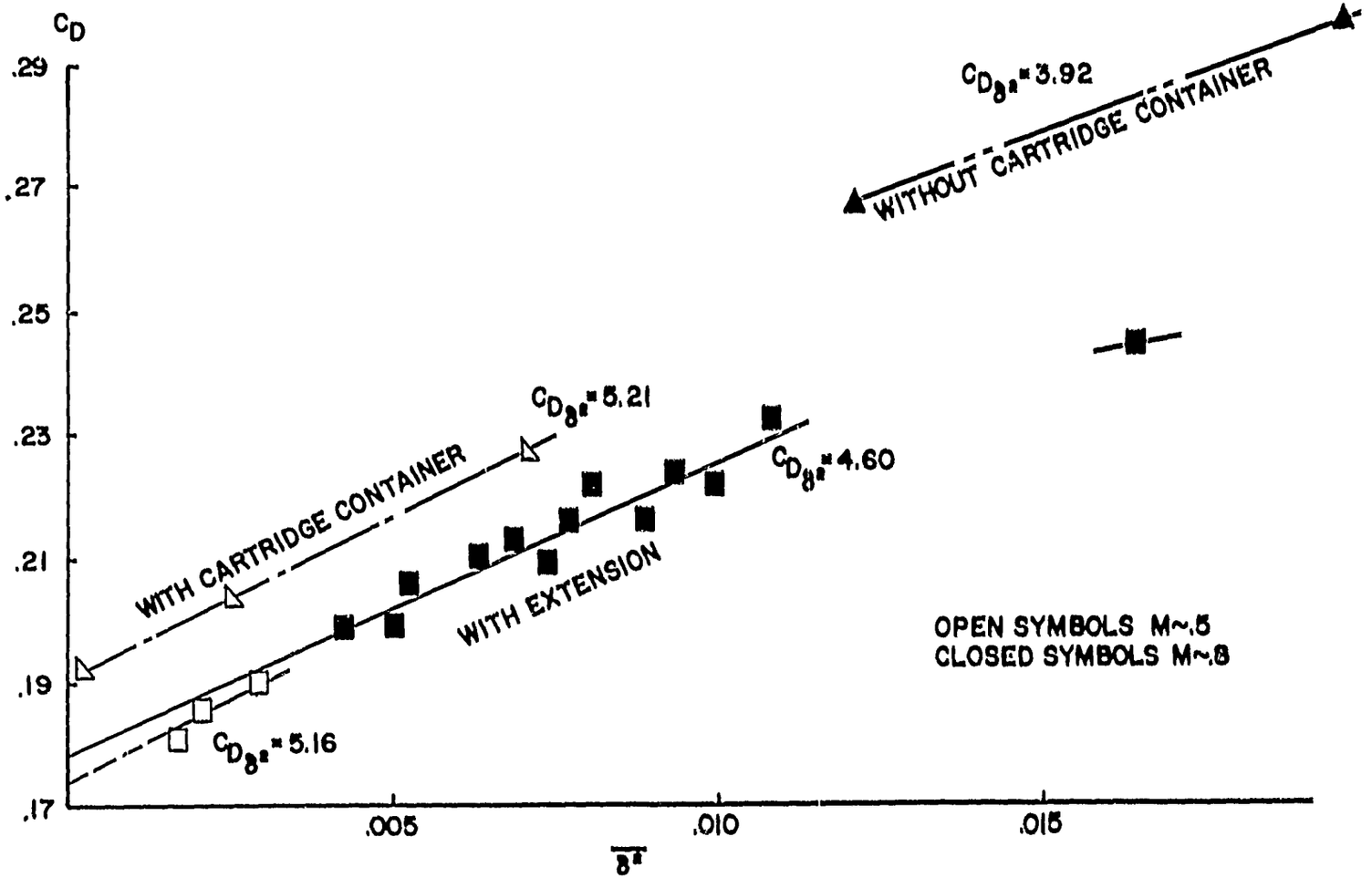

Figure 11. C_D, Square Base Projectile

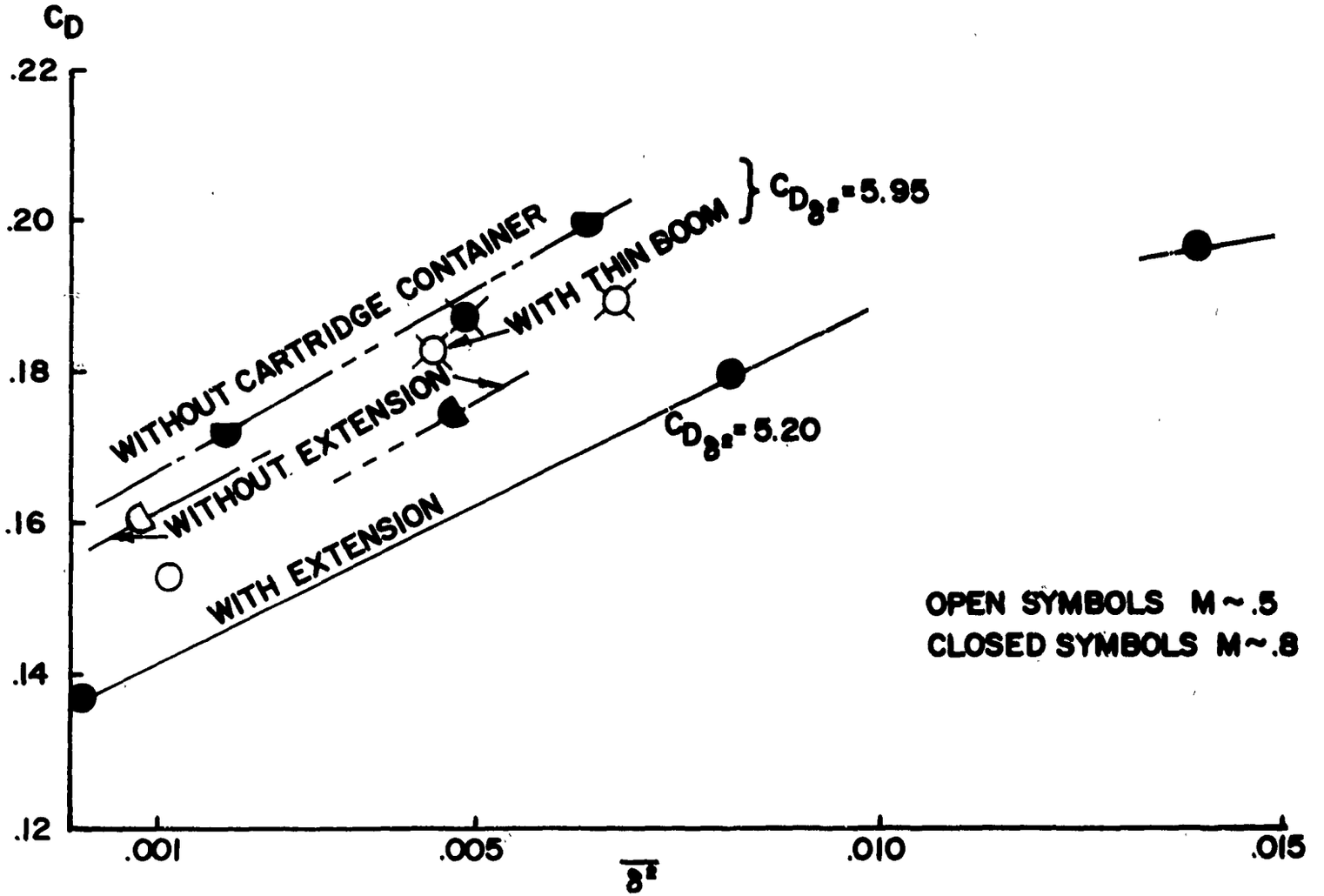

Figure 12. C_D, Boat Tail Projectile

B. Static Moment Coefficient Properties

The data for the square base projectiles with extension at $M \sim .8$ permitted the development of an equation for the aerodynamic moment coefficient of the form:

$$(C_M)_{Static} = (C_{M_{\alpha_o}} + c_2 \delta^2) \delta \qquad (2)$$

through the technique of fitting the $(C_{M_\alpha})_R$, determined from the linearized fit of the range data, as a function of an average yaw parameter for the flight by least squares. This gave values of $C_{M_{\alpha_o}} = 3.93$ and $c_2 = -2.9$. These data and those of the other square base shell are plotted in Figures 13 and 14 as a function of the effective yaw parameter of the test, δ_e^2. A line fit on this form of graph yields an intercept that is the $C_{M_{\alpha_o}}$ term and a slope which is the c_2 coefficient in the above equation. The analytical fitting line for the square base shell at $M \sim .8$ is given and the remainder are graphical. Three points for square base rounds with extension at $M \sim .5$ indicate a higher slope and intercept but the absence of data overlap in these two groups prevents determination of whether this is a Mach number effect or whether this indicates a more complex yaw behavior with no Mach number influence. $(C_{M_\alpha})_R$ for the remaining types, those without extension and those without cartridge container, are also isolated in both Mach number and yaw level. The analytical value of c_2 previously determined can be passed through each group with good representation. Various base fixtures change the center of mass of the assembly slightly. The moment coefficient slope of the shell with extension is considerably higher than those of the others and correction to an identical center of mass position does not reduce this difference significantly. Thus, the principal effect of the extension in the increase of C_{M_α} is aerodynamic in nature. A similar adjustment to the data for the other types superimposes the results. Although these two groups of data are not at the same Mach number, this

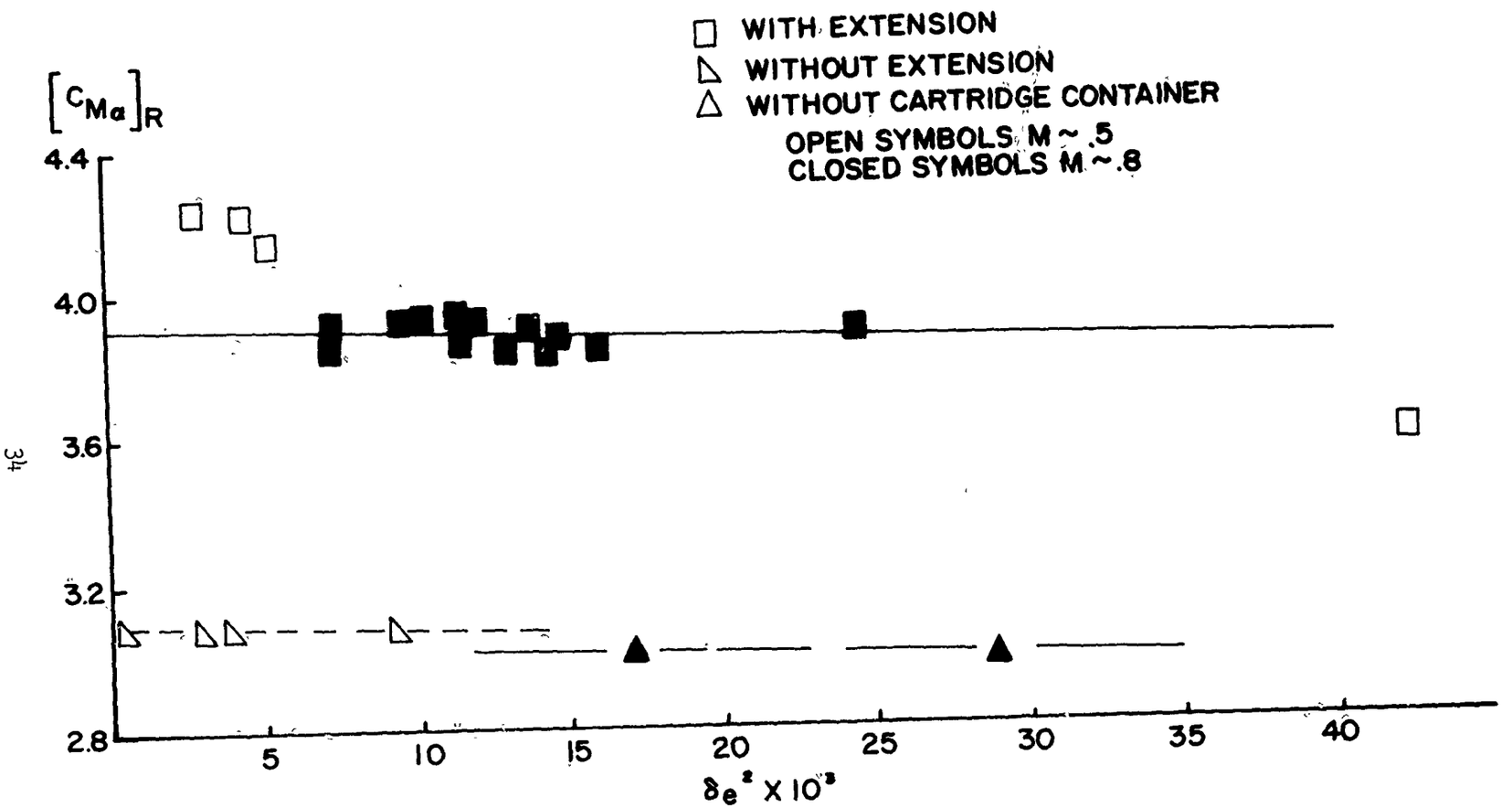

Figure 13. $(C_{M_\alpha})_R$, Square Base Projectile

suggests that the effect of the cartridge container alone is primarily a mechanical shift of the center of mass of the shell.

Data for the boat tail shell are sparse and a reasonable determination of the influence of yaw is possible only for the shell with extension at M ~ .8. The general pattern is very similar to that of the square base shell, however; the shell with extension produce a higher value of C_{M_α} and the difference is predominantly aerodynamic, the slope of these data is at least compatible with the remaining groups, and the differences between the shell with and without cartridge container are small. A special thin boom was tested on the boat tail shell, Figure 4, which had the length of the normal cartridge container plus extension but was of smaller diameter. These data lie between those of the shell with normal cartridge container and those of the shell with extension. For the boat tail shell the magnitude of the change due to the extension is only slightly larger than that which occurred for the square base version. In general, the boat tail projectiles have about a ten per cent higher over-turning moment value than the square base shell.

The lift curve slope, C_{L_α}, is shown in Figure 15. This coefficient is not well determined at small yaws because of the small amplitude of the swerving motion in these cases. Except for a weak decreasing trend at the higher yaw levels, there is little to distinguish the data for various levels of yaw, Mach number or types of projectiles. The M ~ .5 data for the square base shell with extension do lie below the level of the M ~ .8 data but are also at lower yaw levels and poorly determined. Apart from this aberration, a C_{L_α} value of about 1.9 could represent all of the better data below about six degrees of yaw. For the boat tail projectiles, the lift curve slope appears to increase with the square of the effective yaw as determined by the three data points representing the shell with extension at M ~ .8. The remaining configurations present too few data to establish trends.

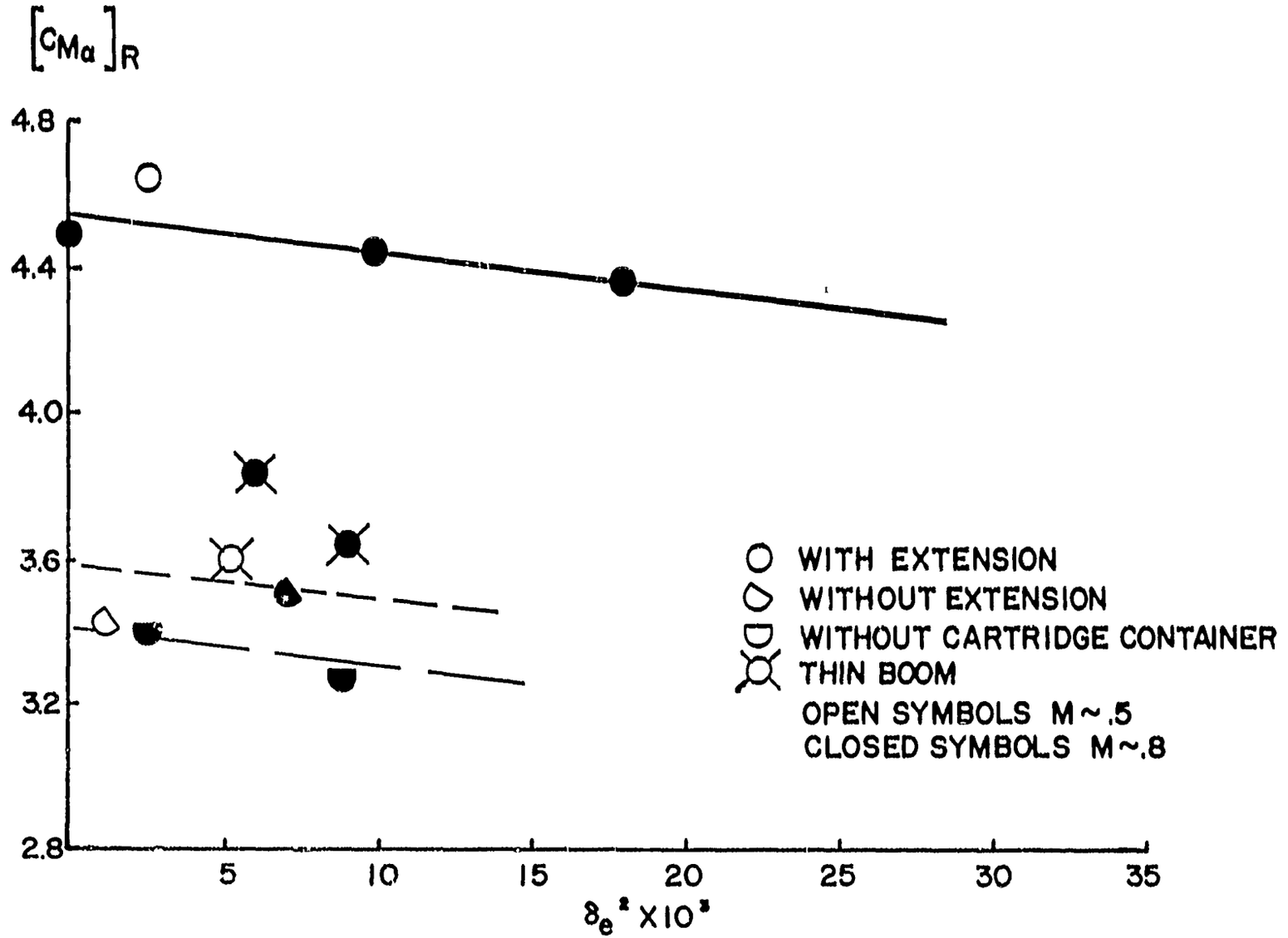

Figure 14. $(C_{M_\alpha})_R$, Boat Tail Projectile

Since the moment coefficient was very sensitive to the addition of the extension and the force coefficient was not, the result implies a change in the center of pressure location. The center of pressure of the normal forces lies about .6 caliber more forward for the square base shell with extension than it does for the other square base shell.

C. Magnus and Damping Moment Coefficients

The coefficients denoted as $C_{M_{p\alpha}}$ and $(C_{M_q} + C_{M_{\dot{\alpha}}})$ derived from the range data are basically obtained from the damping factors, λ_i, which result from fitting the epicyclic yaw equation to the measured yawing motion data. The epicyclic yaw equation and its associated λ parameters are a solution to the linearized equation of the yawing motion:

$$\tilde{\xi}'' + (H - iP)\,\tilde{\xi}' - (M + iPT)\,\tilde{\xi} = 0 \,. \qquad (3)$$

If the coefficients of $\tilde{\xi}'$ and $\tilde{\xi}$ in the differential equation describing the actual yawing motion are nonlinear with yaw amplitude, the linear aerodynamic coefficients deduced from the fit of the epicyclic solution of the linear equation to the actual data will also show nonlinearities. However, nonlinearities in particular aerodynamic terms influence and interact with the linearized fit coefficients normally associated with other aerodynamic terms. Therefore, with nonlinearities in either the Magnus or damping moment slopes, it is convenient to analyze these unrelated aerodynamic properties together since the interacting parameters from the linearized fit can then be considered simultaneously in order to distinguish between the basic aerodynamic variations.

These $(C_{M_{p\alpha}})_R$ and $(C_{M_q} + C_{M_{\dot{\alpha}}})_R$ coefficients from the fits of the data for all the types tested indicated that some nonlinearity was present. In the case of the square base projectile with extension, and only in this case, there were sufficient data to indicate that not only was a nonlinearity present but that it was other than the cubic. The case of the cubic moments has been reported[2] and is usually treated in terms of the variations of the derived coefficient terms $(C_{M_{p\alpha}})_R$ and

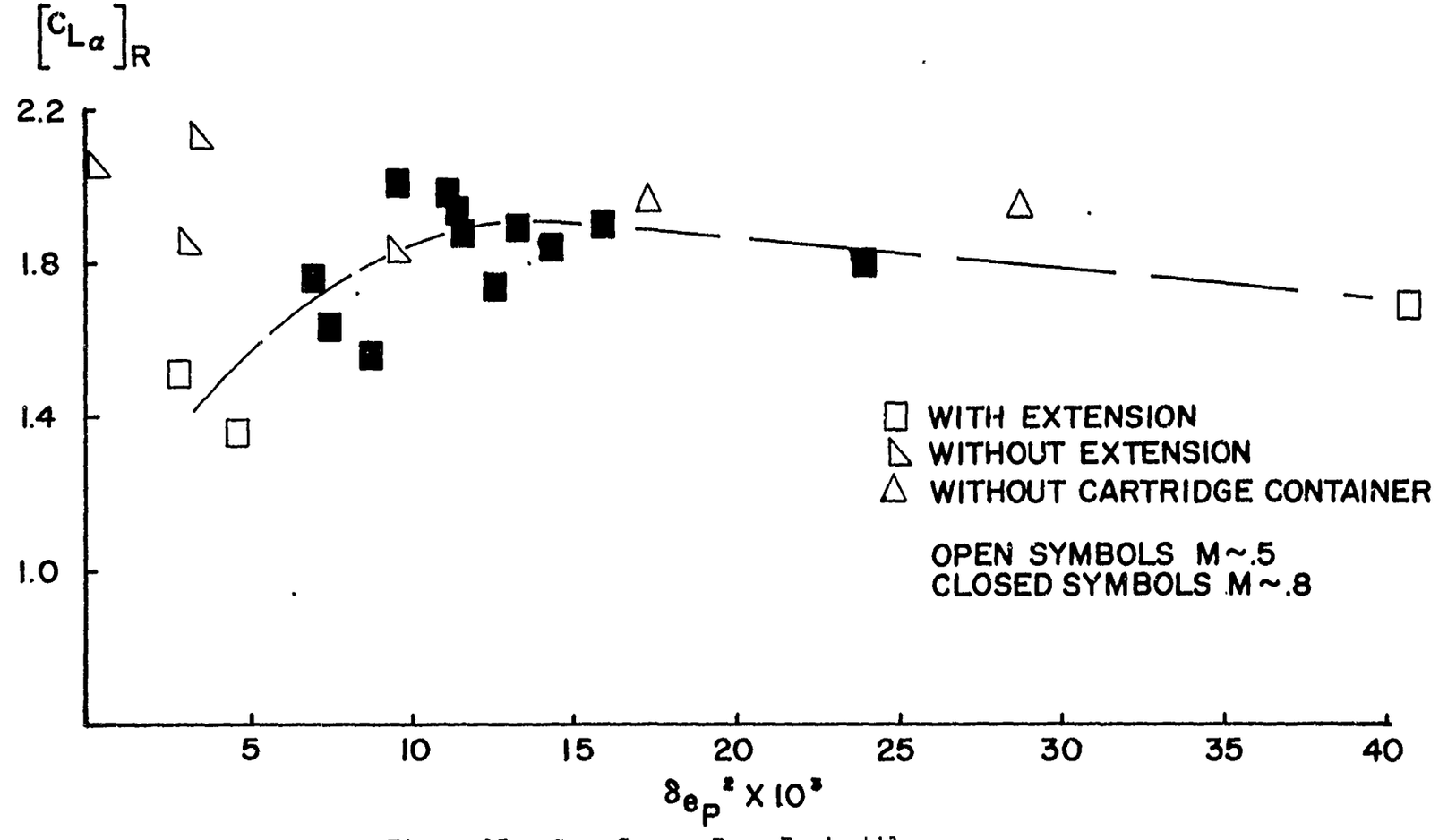

Figure 15. C_{L_α}, Square Base Projectiles

$(C_{M_q} + C_{M_{\dot{\alpha}}})_R$ with effective yaw variables. For the more detailed investigation of the higher order nonlinearity indicated by the plotted results, the damping factors themselves are used since they are directly determined from the yawing motion fit.

The basic theory underlying the analysis by means of the damping factors is identical to that which is applied when the linearized aerodynamic terms are analyzed with respect to the effective yaw parameters. Since the damping factor approach is less familiar, the more pertinent relationships will be reviewed.

If only the Magnus moment is nonlinear and is cubic in yaw level[2],

$$(C_M)_{Magnus} = (C_{M_{p_{\alpha_o}}} + \hat{c}_2 \delta^2) \delta \left(\frac{pd}{V}\right) \tag{4}$$

and the comparable relation for the damping factors is

$$\lambda_i = \lambda_{i0} + \lambda_{i2} (\delta^2)_{ei} \tag{5}$$

where "i" is either N or P. For this particular case $\lambda_{N2} = -\lambda_{P2}$ and the slopes of the λ_i on the effective yaw plot are equal in magnitude but opposite in sign. This is not the case if damping moment nonlinearities are involved, either alone or in combination with a Magnus moment nonlinearity. The λ_i data for the square base projectiles with extension show a mirror image pattern, but one that has a higher order than linear when plotted versus δ^2_{ei}. This suggested that only a Magnus moment nonlinearity was involved.

For a higher order nonlinearity of the Magnus moment

$$(C_M)_{Magnus} = (\hat{c}_o + \hat{c}_2 \delta^2 + \hat{c}_4 \delta^4 + \ldots\ldots) \delta \left(\frac{p\,d}{V}\right) \tag{6}$$

and the resulting damping factor expression[5] is

$$\lambda_i = \lambda_{io} + \lambda_{i2} (\delta^2)_{ei} + \lambda_{i4} (\delta^4)_{ei} + \ldots\ldots\ldots \tag{7}$$

In this expression the λ_{i2} and λ_{i4} coefficients are also equal in magnitude and opposite in sign for λ_N and λ_P. However, although the $(C_M)_{Magnus}$ variation is polynomial in the aerodynamic yaw, the λ_i expressions in terms of the effective yaw parameters, which are averaging quantities, are not since:

$$(\delta^4)_{ei} \neq \left[(\delta^2)_{ei}\right]^2$$

Thus, the relations between the λ_{i2} and λ_{i4} coefficients must be established by fitting the data analytically.

If this equal and opposite variation of the higher order coefficients is established, it is not only proven that the only nonlinearity is in the Magnus moment and that it is polynomial in yaw to the degree of the fit required in treating the λ data; but the parameters of the λ fit also can be used in determining the terms in the Magnus moment coefficient expansion and the constant value of $(C_{M_q} + C_{M_{\dot{\alpha}}})$.

$$(C_{M_{p\alpha}})_o = k_a^2 \left[- \frac{2\,m}{\rho\, S\, d} \left(\frac{\lambda_{NO}\, \phi_P' + \lambda_{PO}\, \phi_N'}{\phi_P' + \phi_N'} \right) - C_{L_\alpha} \right] \tag{8}$$

$$\hat{c}_2 = k_a^2 \left[\frac{2\,m}{\rho\, S\, d} \left(\frac{\phi_N' - \phi_P'}{\phi_P' + \phi_N'} \right) \lambda_{N2} \right]$$

$$\hat{c}_4 = k_a^2 \left[\frac{2\,m}{\rho\, S\, d} \left(\frac{\phi_N' - \phi_P'}{\phi_P' + \phi_N'} \right) \lambda_{N4} \right]$$

and $$(C_{M_q} + C_{M_{\dot{\alpha}}}) = k_t^2 \left[C_{L_\alpha} - C_D + \frac{2\,m}{\rho\, S\, d} (\lambda_{NO} + \lambda_{PO}) \right] . \tag{9}$$

With the data for the square base projectile with extension in the $M \sim .8$ range the nutational and precessional damping rates were first fitted by least squares independently. The results were:

$\lambda_{N0} = + .484 \times 10^{-3}$ 1/cal $\quad \lambda_{P0} = - .987 \times 10^{-3}$ 1/cal

$\lambda_{N2} = - .073$ 1/cal $\quad \lambda_{P2} = + .078$ 1/cal

$\lambda_{N4} = + 1.65$ 1/cal $\quad \lambda_{P4} = - 1.79$ 1/cal

$\sigma_{fit} = .563 \times 10^{-3}$ 1/cal $\quad \sigma_{fit} = .118 \times 10^{-3}$ 1/cal

Since $\lambda_{N2} = - \lambda_{P2}$ and $\lambda_{N4} = - \lambda_{P4}$ to well within the accuracy of the data fit, the conditions for only a Magnus moment nonlinearity are satisfied and terms of order higher than $(\delta^4)_{ei}$ are not needed for the range of yaw $\alpha_t < 11°$. The λ_P and λ_N data were then fitted simultaneously with the constraint that $\lambda_{N2} = - \lambda_{P2}$ and $\lambda_{N4} = - \lambda_{P4}$ to obtain the final coefficients. These results were:

$\lambda_{N0} = + .496 \times 10^{-3}$ 1/cal

$\lambda_{P0} = - .782 \times 10^{-3}$ 1/cal

$\lambda_{N2} = - .075$ 1/cal

$\lambda_{N4} = + 1.72$ 1/cal

$\sigma_{fit} = .123 \times 10^{-3}$ 1/cal

This enforced antisymmetry of the λ_{i2} and λ_{i4} coefficients produces only a slightly larger error of fit than the better of the two separate fits.

The aerodynamic coefficients derived from this fit are:

$$(C_M)_{Magnus} = (1.38 - 143\ \delta^2 + 3300\ \delta^4)\ \delta \left[\frac{p\ d}{V}\right] \qquad (10)$$

$$(C_{M_q} + C_{M_{\dot{\alpha}}}) = - 8.13 \qquad (11)$$

and are valid for these data for the yaw range to approximately six degrees. The analysis applied to the data for the square base projectiles with extension was possible because the number of data points was

adequate to support a statistical fit of the data. There was insufficient data available for similar treatment of the remaining six configurations. For these projectiles it is necessary to presume the yaw variation in order to present the data. It will be assumed, on the basis of the analytical case, that all the other test configurations share the property that only the Magnus moment, and not the damping moment derivative sum, is nonlinear with yaw. The amount of data permits only consideration of a cubic assumption. If the aerodynamic Magnus moments were to vary as:

$$(C_M)_{Magnus} = (C_{M_{p\alpha_o}} + \hat{c}_2 \delta^2) \delta \left(\frac{p d}{V}\right) \tag{12}$$

and the damping moments were constant,

$$C_{M_q} + C_{M_{\dot{\alpha}}} = \text{constant} \tag{13}$$

then the range determined value of the Magnus moment slope, $(C_{M_{p\alpha}})_R$, would vary as:

$$(C_{M_{p\alpha}})_R = C_{M_{p\alpha_o}} + \hat{c}_2 (\delta^2)_e \tag{14}$$

and $(C_{M_q} + C_{M_{\dot{\alpha}}})_R$ would vary as:

$$(C_{M_q} + C_{M_{\dot{\alpha}}})_R = (C_{M_q} + C_{M_{\dot{\alpha}}}) + \hat{c}_2 (\delta^2)_{e*} \tag{15}$$

where $(\delta^2)_e$ and $(\delta^2)_{e*}$ are average yaw parameters of the individual test. The intercepts with the zero axis of these two plots represent the zero yaw value of the Magnus moment slope $(C_{M_{p\alpha}})_o$ and the true constant value of $(C_{M_q} + C_{M_{\dot{\alpha}}})$ for the range of yaws considered. The variation indicated by $\hat{c}_2$ in the last equation is not an indication of the variation of the damping moment with yaw but only serves as a device to correct the linearized results of the range data fit.

In Figure 16, the data for the square base designs are plotted as a function of the effective yaw level, $(\delta^2)_e$. The previous analytical determination for the projectile with extension is given to show the nature of this higher order variation as a background for the remaining types. In order to plot an analytic curve from the quartic fit equation as a function of $(\delta^2)_e$ alone it is necessary to select a particular type of motion to define the $(\delta^4)_e$ term in terms of $(\delta^2)_e$. The motion with equal nutational and precessional modes was selected as the basis and, for this case, $(\delta^4)_e = \frac{10}{9}[(\delta^2)_e]^2$.

Thus, the solid curve in Figure 16 represents the expected value of $(C_{M_{p_\alpha}})$ reduced from a group of hypothetical test rounds having equal epicyclic arms. Many of the range test rounds approximate this condition but the curve cannot be considered directly as a fit of the actual data which are also plotted. The curve based on the square base projectile with extension shows a steep descent to negative values at yaw angles of about 7°, a flattening out, and then reversal of curvature in the 9° region--indicating that the higher order term will eventually dominate. High positive Magnus moment values would be expected at both small and large yaw.

The data for the other conditions seem to show weaker variations but do not exhibit a complete picture in any case. The data for the square base shell without extension are at $M \sim .5$ and are concentrated in the small yaw region. These show approximately a linear variation in the $(C_{M_{p_\alpha}})$ versus $(\delta^2)_e$ plot which over this small range of yaw ($0° < \alpha_t < 6°$) would be represented by equation 14. The data for the shell without cartridge container consisted of two points, both at $M \sim .8$; one at a yaw level greater than that of the shell without extension and the other at the upper limit of the shell with extension. These have a near zero, but negative, value that changes little with yaw level. Thus, over this range the Magnus moment is linear with yaw and the indicated range value is $(C_{M_{p_\alpha}})_o$. The data for all the square base

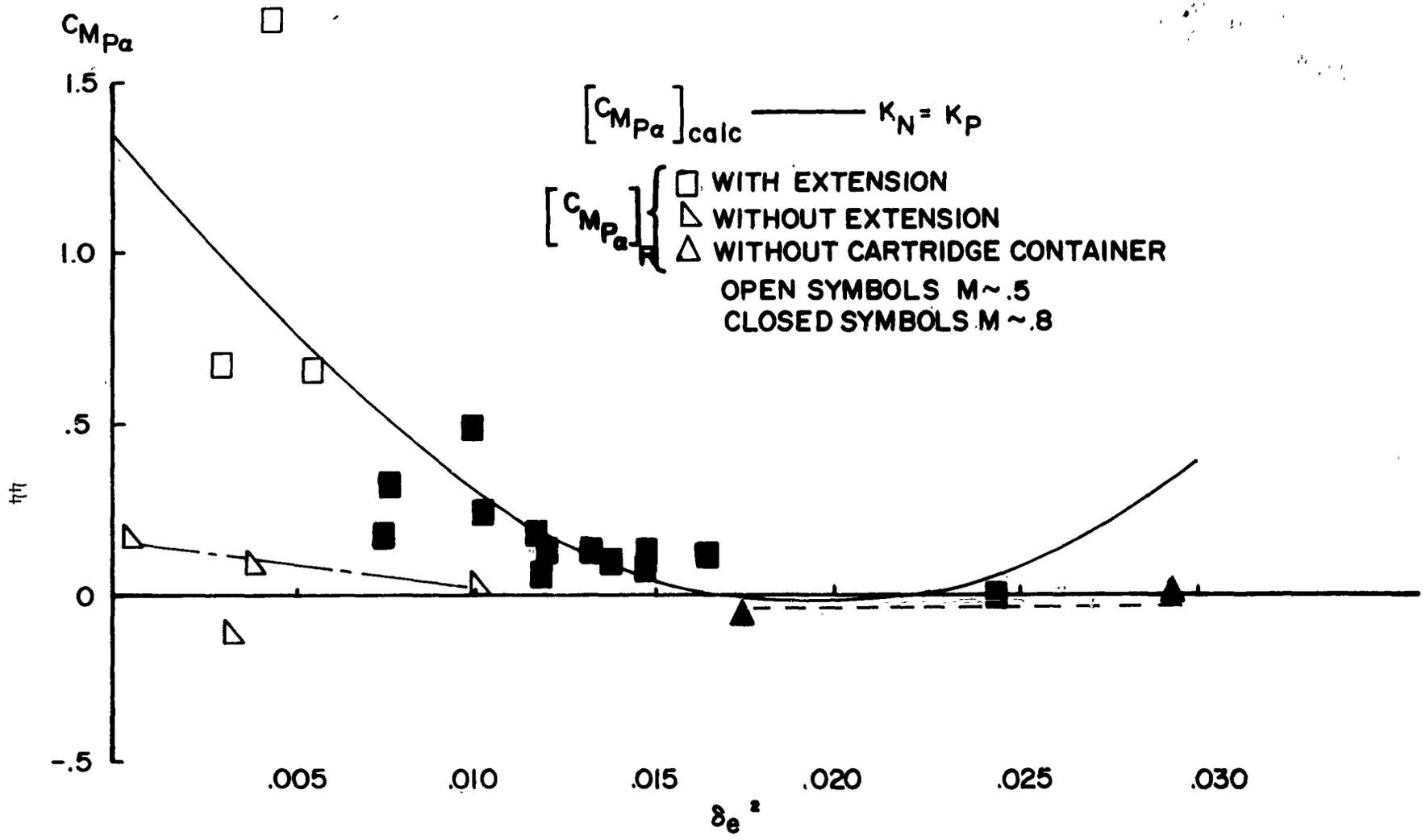

Figure 16. $(C_{M_{p\alpha}})_R$, Square Base Projectile

designs seems to converge at about five degrees of yaw. Except in a few cases, this is the upper limit of the yaw level for these tests.

In Figure 17, which presents the Magnus moment slope for the boat tail projectiles, the few data suggest trends similar to those of the square base designs. The data for the shell with extension show high positive values at small yaw and a decreasing curving trend; the shell without extension and those without cartridge container yield data with smaller values of $(C_{M_{p_\alpha}})_R$ at small yaw and less indication of variation with yaw. The data from the boat tail projectile with special thin boom indicate possible differences which do not define a consistent Mach number or yaw variation but the derived values from the fit of the range data are the most negative of those measured.

The most interesting features of the Magnus data are the marked nonlinearity of the data for the shell with extension and the general similarity of the data for the square base and boat tail shell with similar empennages. For the inertial characteristics of these shell a large positive value of the Magnus moment slope leads to a divergent precessional yaw mode. Thus, the shell with extension are dynamically unstable at small yaw, dynamically stable at higher yaws and the Magnus data suggest high moments could occur again at still higher yaw levels, which is discussed briefly on pages 47 and 48 of this report. The large differences in behavior as a function of types of boom structure suggest that the aerodynamic influence of the boom dominates the damping behavior of the shell.

The individual round data for $(C_{M_q} + C_{M_{\dot{\alpha}}})_R$ are given in Table II. Variations in these values reflect experimental error and, since they were determined by linear fits, are also biased by the influence of the nonlinear Magnus moment. In the case of the square base shell with extension the previously described damping factor fit established the true value of the $(C_{M_q} + C_{M_{\dot{\alpha}}})$ as a constant over the test range of yaws. Graphing the data for the other square base projectile types suggested

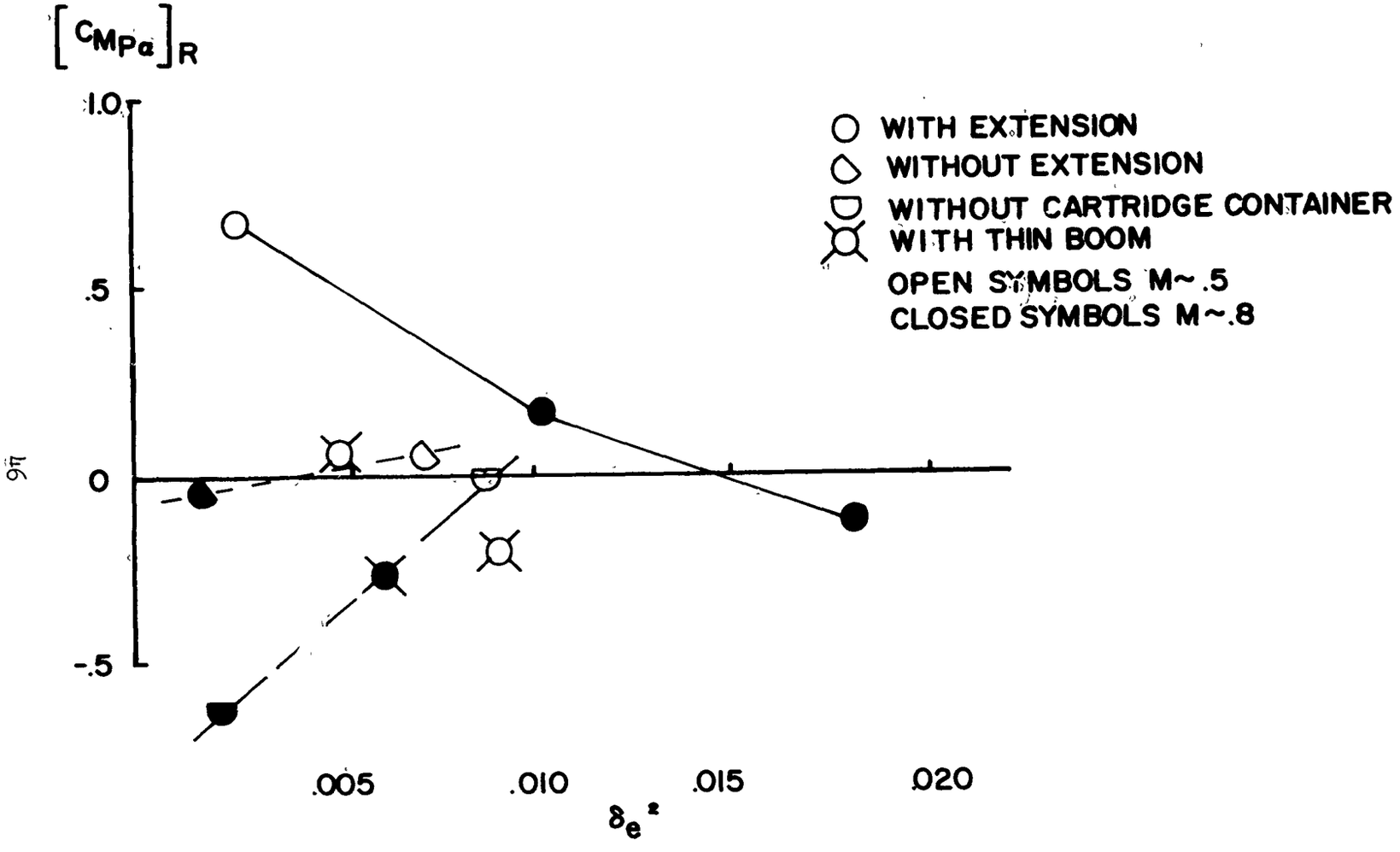

Figure 17. $(C_{M_{p\alpha}})_R$, Boat Tail Projectile

a similar phenomenon and could be extrapolated to a true value with some degree of assurance. The data for the boat tail shell was sparse and there were a maximum of three data points for a given shell at one Mach number. The few data points for each condition were reviewed for quality and the degree of bias expected due to the Magnus variation and on this basis a representative value for each case was selected. These values are given in Table III.

The major features shown are that the values of $(C_{M_q} + C_{M_{\dot{\alpha}}})$ for both the boat tail and the square base shell with similar empennages are comparable, and the shell with or without cartridge container exhibit similar damping coefficient levels in all cases. The shell with extension shows damping coefficients about twice as large as those of the other cases.

Table III. Table of Damping Coefficients

Type Projectile		$C_{M_q} + C_{M_{\dot{\alpha}}}$	Mach No.	Method of Determination	Number of Data Points
Square Base	With Extension	- 8.1	.8	Analytical	13
	Without Extension	- 4.5	.5	Graphical	4
	Without Cartridge Container	- 3.5	.7	Graphical	2
Boat Tail	With Extension	-10.0	.8	Selection	3
	Without Extension	- 3.0	.8	Selection	2
	Without Cartridge Container	- 6.0	.8	Selection	2
	With Thin Boom	- 5.5	.8	Selection	3

The variation of the damping factors with effective yaw for the square base shell with extension indicates that the precessional yaw mode damps and that the nutational mode diverges for small yaw levels.

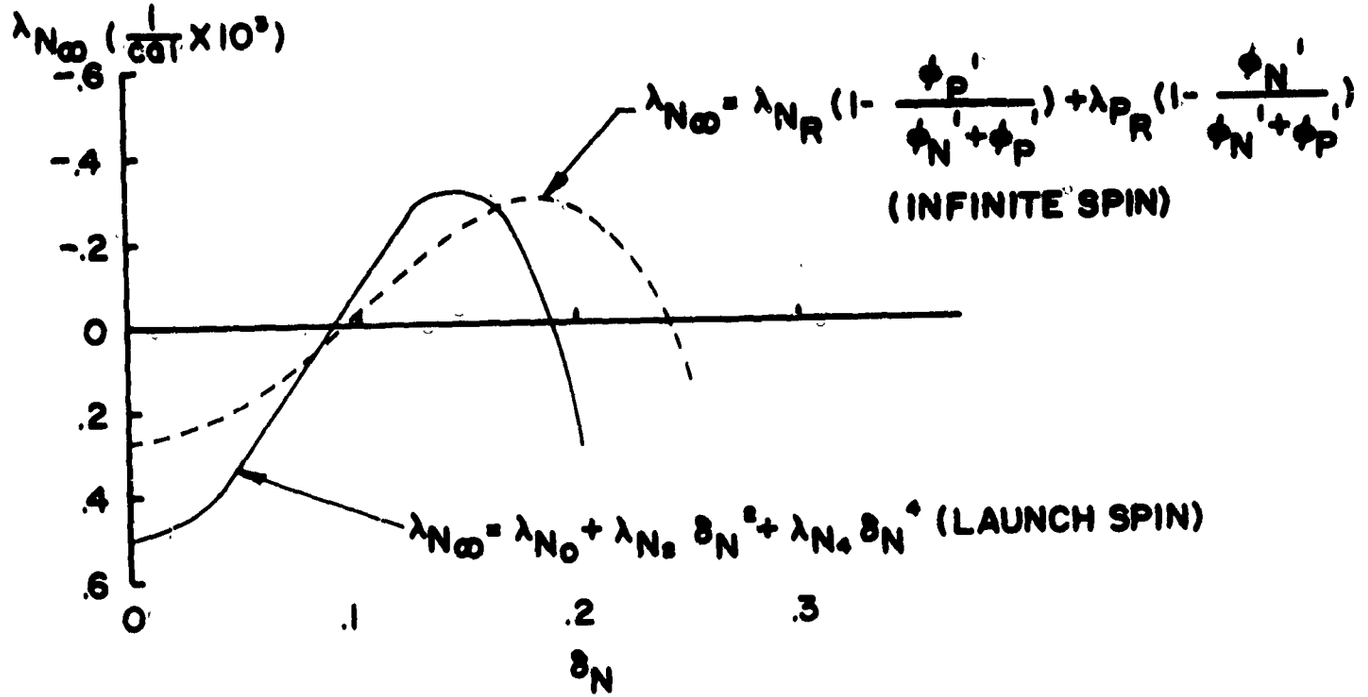

Figure 18. Nutational Damping Factor Range

At higher yaws, both modes damp. This would result in a circular yaw limit cycle for the nutational mode. The fitting equation for λ_N can be used to compute the damping factor as a function of yaw level for the conditions at launch assuming pure nutational yaw. The equation can also be modified to compute λ_N for the case of an infinite stability factor. The actual values of λ_N for almost all proposed mortar trajectories are bounded by these two determinations, and these two curves are plotted as Figure 18. Zero yaw values for λ_N are different but the cross-over points to damped behavior for the two cases are very close, 5.2 and 5.7 degrees yaw, which indicates a general residual motion of the projectile of about $5\frac{1}{2}$ degrees yaw. The first zero point of the λ_N curve is interior to the range of the data used in the fit and is quite reliable. The existence of the higher order term in the Magnus moment variation produces a second intercept with the zero axis at higher yaws. This indicates that the projectile could again become dynamically unstable at yaw levels above those of this test. In the case of the launch condition curve this is indicated at about eleven degrees and for the limiting case at about $12\frac{1}{2}$ degrees. The second zero damping point involves an extrapolation of the fitting curve beyond the range of the test data and must be considered speculative.

IV. SUMMARY

Some variations of two versions of the XM 571 RAC 107mm spin stabilized mortar projectiles, without rocket assist, were evaluated by free flight range testing. The two principal modifications of the 18.28 caliber secant ogival nosed configuration were the presence of a boat tail rather than a square base, and the addition of the extension to the starting cartridge container. A small number of rounds were fired with a long thin starting cartridge container and others without any base appendage. The tests covered a yaw range up to about 10° but were restricted to two Mach numbers, $M \sim .8$ and $M \sim .5$, with half of the data points representing the shell with the square base and extension.

The general influence of the extension on the aerodynamic properties is to produce a lower drag, higher static moment, strongly nonlinear Magnus moment and large damping moment coefficient. Those shell without extension indicated a lower drag than those without cartridge container, but there was no essential difference between these groups in static moment, Magnus moment or damping coefficient. From the data available, the boat tail and the square base projectile show similar performance except that the drag is lower for the boat tail shell and the static moment coefficient is characteristically higher.

For the shell with extension, the high Magnus moment at small yaw is sufficient to induce a divergence of yaw while at higher yaw the lower value of $C_{M_{p\alpha}}$ permits damping. Hence, a small limit cycle yawing motion will normally result.

REFERENCES

1. W. K. Rogers, "The Transonic Free Flight Range," Ballistic Research Laboratories Report No. 1044, June 1958, AD 200177.

2. C. H. Murphy, "Free Flight Motion of Symmetric Missiles," Ballistic Research Laboratories Report No. 1216, July 1963, AD 442757.

3. E. R. Dickinson, "Physical Measurements of Projectiles," Ballistic Research Laboratories Technical Note No. 874, February 1954, AD 803103.

4. C. H. Murphy, "The Measurement of Nonlinear Forces and Moments by Means of Free Flight Tests," Ballistic Research Laboratories Report No. 974, February 1956, AD 93521.

5. C. H. Murphy, "Prediction of the Motion of Missiles Acted on by Nonlinear Forces and Moments," Ballistic Research Laboratories Report No. 995, October 1956, AD 122221.

UNCLASSIFIED

Security Classification

DOCUMENT CONTROL DATA - R & D

(Security classification of title, body of abstract and indexing annotation must be entered when the overall report is classified)

1. ORIGINATING ACTIVITY (Corporate author) U.S. Army Aberdeen Research and Development Center Ballistic Research Laboratories Aberdeen Proving Ground, Maryland	2a. REPORT SECURITY CLASSIFICATION Unclassified 2b. GROUP

3. REPORT TITLE

ANALYSIS OF FREE FLIGHT TESTS OF 107MM MORTAR PROJECTILE XM 571 RAC

4. DESCRIPTIVE NOTES (Type of report and inclusive dates)

5. AUTHOR(S) (First name, middle initial, last name)

William D. Donovan

6. REPORT DATE	7a. TOTAL NO. OF PAGES	7b. NO. OF REFS
October 1969	54	5

8a. CONTRACT OR GRANT NO. b. PROJECT NO. RDT&E 1T262301A201 c. d.	9a. ORIGINATOR'S REPORT NUMBER(S) Memorandum Report 2013 9b. OTHER REPORT NO(S) (Any other numbers that may be assigned this report)

10. DISTRIBUTION STATEMENT

This document is subject to special export controls and each transmittal to foreign governments or foreign nationals may be made only with prior approval of Commanding Officer, U.S. Army Aberdeen Research and Development Center, Aberdeen Proving Ground,

11. SUPPLEMENTARY NOTES	12. SPONSORING MILITARY ACTIVITY
	U. S. Army Materiel Command Washington, D. C.

13. ABSTRACT

Free flight aerodynamic range data are presented for the 107mm XM 571 RAC mort projectile in unboosted configuration. Seven different models were tested and of the data was obtained for the square base shell with extension. For M ~ 0.[illegible] within the small yaw region, this projectile developed a quintic Magnus moment. was established that the length of the base attachment (extension) directly inf[illegible] the values of the aerodynamic coefficients.

DD FORM 1 NOV 68 1473 REPLACES DD FORM 1473, 1 JAN 64, WHICH IS OBSOLETE FOR ARMY USE.

UNCLASSIFIED

Security Classification

14. KEY WORDS	LINK A		LINK B		LINK C	
	ROLE	WT	ROLE	WT	ROLE	WT
Aerodynamic Characteristics						
Nonlinear Magnus Moments						
Heavy Mortar Shell						
Base Attachments						
Damping Factor Analysis						